Published in final edited form as:
Ultrasound Med Biol. 2011 August ; 37(8): 1240–1251. doi:10.1016/j.ultrasmedbio.2011.05.011.

ULTRASOUND-ENHANCED rt-PA THROMBOLYSIS IN AN *EX VIVO* PORCINE CAROTID ARTERY MODEL

Kathryn E. Hitchcock[*], **Nikolas M. Ivancevich**[*], **Kevin J. Haworth**[*], **Danielle N. Caudell Stamper**[†], **Deborah C. Vela**[‡], **Jonathan T. Sutton**[*], **Gail J. Pyne-Geithman**[†], and **Christy K. Holland**[*]

[*]Department of Internal Medicine, Division of Cardiovascular Diseases and Biomedical Engineering Program, University of Cincinnati, Cincinnati, OH

[†]Department of Neurosurgery, University of Cincinnati, Cincinnati, OH

[‡]Texas Heart Institute, Houston, Texas

Abstract

Ultrasound is known to enhance recombinant tissue plasminogen activator (rt-PA) thrombolysis. In this study, occlusive porcine whole blood clots were placed in flowing plasma within living porcine carotid arteries. Ultrasonically induced stable cavitation was investigated as an adjuvant to rt-PA thrombolysis. Aged, retracted clots were exposed to plasma alone, plasma containing rt-PA (7.1 ± 3.8 μg/mL) or plasma with rt-PA and Definity® ultrasound contrast agent (0.79 ± 0.47 μL/mL) with and without 120-kHz continuous wave ultrasound at a peak-to-peak pressure amplitude of 0.44 MPa. An insonation scheme was formulated to promote and maximize stable cavitation activity by incorporating ultrasound quiescent periods that allowed for the inflow of Definity®-rich plasma. Cavitation was measured with a passive acoustic detector throughout thrombolytic treatment. Thrombolytic efficacy was measured by comparing clot mass before and after treatment. Average mass loss for clots exposed to rt-PA and Definity® without ultrasound (n = 7) was 34%, and with ultrasound (n = 6) was 83%, which constituted a significant difference (p < 0.0001). Without Definity® there was no thrombolytic enhancement by ultrasound exposure alone at this pressure amplitude (n = 5, p < 0.0001). In the low-oxygen environment of the ischemic artery, significant loss of endothelium occurred but no correlation was observed between arterial tissue damage and treatment type. Acoustic stable cavitation nucleated by an infusion of Definity® enhances rt-PA thrombolysis without apparent treatment-related damage in this *ex vivo* porcine carotid artery model.

Keywords

Sonothrombolysis; Thrombolysis; rt-PA; Stable cavitation; Vascular bioeffects; Passive cavitation detection; *Ex vivo* vascular model

Address correspondence to: Christy K. Holland, Ph.D., Department of Internal Medicine, Division of Cardiovascular Diseases and Biomedical Engineering Program, CVC 3935, 231 Albert Sabin Way, Cincinnati, OH 45267-0586. Christy.Holland@uc.edu.

INTRODUCTION

Potent thrombolytic agents such as recombinant tissue plasminogen activator (rt-PA) have enabled effective clot lysis in occluded arteries in the brain and other sites, particularly for salvage of cardiac tissue in acute myocardial infarction (Mueller et al. 1985). For ischemic stroke, however, a higher rate of intracranial hemorrhagic complications is associated with higher rt-PA doses in clinical thrombolytic treatment (Cannon 2000). Thus, improved thrombolysis or greater safety could allow physicians to administer rt-PA to a greater portion of patients with ischemic stroke, including some who are now excluded because of concern for hemorrhagic complications. Researchers have examined the ability of ultrasound to enhance the efficacy of thrombolytic agents (Sobbe et al. 1974; Trubestein et al. 1976; Siegel et al. 2000). Investigations by Francis and his coworkers suggest that ultrasound accelerates enzymatic fibrinolysis by increasing transport of reactants through a cavitation-related mechanism (Francis et al. 1992; Blinc et al. 1993; Francis et al. 1995). Several investigators have used low-frequency, low-intensity ultrasound to accelerate rt-PA thrombolysis *in vitro* (Akiyama et al. 1998; Behrens et al. 1999; Saguchi et al. 2008). In addition, mechanistic studies *in vitro* have revealed that stable cavitation is correlated with enhanced rt-PA thrombolysis (Datta et al. 2006, 2008); yet strategies to optimize the occurrence of such bubble activity and avoid potential harmful bioeffects have yet to be identified.

Alexandrov et al. (2004) used 2-MHz transcranial Doppler ultrasound to monitor the middle cerebral artery in acute ischemic stroke patients. These authors observed an increase in the rate of sustained complete recanalization within 2 h after the administration of rt-PA in patients who were also monitored with ultrasound. However, another study carried out in patients using 300-kHz pulsed transcranial ultrasound in combination with rt-PA demonstrated an increased rate of cerebral hemorrhage, prompting the premature cessation of the study (Daffertshofer et al. 2005). Later simulations showed that this trial treatment may have resulted in rarefactional pressures in excess of 1 MPa (Baron et al. 2009) because of the formation of standing waves inside the skull, and exploration of treatments using less vigorous insonation are warranted.

The goal of this work was to determine whether ultrasonic stable cavitation could be sustained using a continuous infusion of a commercial contrast agent, Definity (Lantheus Medical Imaging, N. Billerica, MA, USA) in flowing plasma and to maximize this bubble activity to promote rt-PA thrombolytic enhancement. The study was carried out in living, excised porcine carotid arteries to simulate the cavitational milieu inside the body and allow monitoring of cavitation activity using a hydrophone. In addition, the biological effects of the combined ultrasound and thrombolytic treatments on the *ex vivo* arteries were observed.

MATERIALS AND METHODS

Porcine whole blood clots were formed in glass pipettes, placed within excised porcine carotid arteries and mounted in a flow system within a water tank to allow exposure to 120-kHz ultrasound. Perfusion with oxygen-rich pooled porcine plasma maintained viability of arterial tissue segments and enabled injection of rt-PA and an echo contrast agent, Definity.

This apparatus was designed to allow detection of acoustic cavitation in a vascular environment that closely resembled the body, while permitting control of flow variables (Hitchcock et al. 2010).

Source transducer characteristics and calibration

A circular 120-kHz single-element transducer (Sonic Concepts Inc., Woodinville, WA, USA) with a 6.14-cm diameter was calibrated in water using a 0.5-mm hydrophone (Reson, TC 4038, Goleta, CA, USA) mounted on a computer-controlled three-axis positioner (Velmex, NF-90 series, Bloomfield, NY, USA). The transducer had a −3-dB beam width of 2.5 cm and a Rayleigh distance of 10.4 cm. The 120-kHz transducer was driven with a function generator (Agilent, 33120A, Palo Alto, CA, USA), power amplifier (75A250, AR Amplifier Inc., Souderton, PA, USA) and custom-built impedance matching network (Sonic Concepts Inc.).

The ex vivo flow system

The carotid arteries of 38 mature domestic pigs (6 to 10 months old) were excised within 20 min of exsanguination at an abattoir. The arteries were rinsed with cool (15°C) phosphate-buffered saline (PBS; Fisher Scientific, Hampton, NH, USA) to remove free blood and then stored in individual plastic bags in ice-cold PBS until use. All arteries were used within 72 h of excision (Thorne and Paul 2003). Whole blood was collected from abattoir pigs during exsanguination and immediately transferred to 1.9-mL Pasteur pipettes with tips sealed using surgical wax. The blood-filled pipettes were covered and incubated in a 37°C water bath for 3 h, and stored at 4°C for at least three days before use to allow clot retraction (Shaw et al. 2001; Holland et al. 2002; Datta et al. 2006). Fully retracted clots are more difficult to lyse with rt-PA and are typical of thrombi that have matured over prolonged periods in the heart (Marcu et al. 2007). These types of thrombi usually occur in the left atrium during atrial fibrillation and can lead to ischemic stroke. The relative resistance of clots to rt-PA thrombolysis *in vivo* is related to their origin and composition and varies widely (Undas et al. 2006a, 2006b; Mutch et al. 2010; Boulaftali et al. 2011). The choice of fully retracted clots for use in our study, though structurally different than some clots *in vivo*, is aimed at a worst-case scenario.

Each artery was weighed, and a clot was cut to 3.2 cm in length, weighed, gently injected into a 4.4-cm length of carotid artery and mounted in a special-purpose-built stainless steel and Delrin frame using 1/8 inch polypropylene barb-style tubing fittings as cannulae (EW-45500-34, Cole-Parmer, Vernon Hills, IL, USA). An acoustically transparent latex wall was placed around the frame to make an enclosed, leak-proof chamber, and the space between latex and artery was filled with degassed (1.73 ± 0.5 mg O_2/L) artificial cerebrospinal fluid (aCSF) to simulate the environment of the middle cerebral artery. The aCSF was composed of 128 NaCl, 3.0 KCl, 1.0 $MgSO_4$, 23.5 $NaHCO_3$, 0.5 NaH_2PO_4 and 30 glucose, all in mMol/L (Kehr et al. 2001). The cannulae were connected to a flow system through which 37 °C, citrated, oxygenated porcine plasma (Lampire Biological Products, Pipersville, PA, USA) circulated with a reciprocating pump as described by Hitchcock et al. (2010). The temperature of the plasma was maintained at 37 ± 0.5°C, the pH was 7.37 ± 0.03 and the dissolved oxygen content of the plasma was sustained at 23.3 ± 1.5 mg/L using

a mixture of 95% oxygen and 5% carbon dioxide *via* semipermeable tubing. Pressure in the carotid artery was kept between 90 and 110 mm Hg, which is physiologic for both humans and domestic pigs (Pond and Mersmann 2001; Li et al. 2005). B-mode images taken with a Philips HDI 5000 scanner using a C5-2 array (Philips Medical Systems, Bothell, WA, USA) showed that the average clot length in the physiologic flow was 1.9 ± 0.2 cm. Thus, the pressure and flow field compressed the clot lengthwise. Of this length, 1.25 cm was within the −3-dB beam width of the 120-kHz transducer, and 0.4 cm was within the −3-dB beam width of the 2.25 MHz cavitation detection hydrophone.

Table 1 highlights the numbers of arteries in each treatment protocol. Oxygenated plasma flowed through each artery. Either (i) plasma; (ii) plasma plus rt-PA; or (iii) plasma, rt-PA and Definity were injected using an inline catheter placed approximately 30 cm proximal to the artery inlet. The plasma injection into flowing plasma served as the control treatment group. Definity was diluted to a concentration of 1.55 μL/mL in plasma and continuously infused proximal to the artery at a rate of 0.6 mL/min *via* an inline catheter. Injection of Definity upstream of the artery segment was necessary to prevent destruction of the Definity microbubbles by the reciprocating pump. Note that all clots were exposed to endogenous tissue plasminogen activator (t-PA) in the plasma, at an approximate concentration of 8 ng/mL (Jern et al. 1997). The target concentrations of rt-PA and Definity in the artery post injection were 3.15 μg/mL (Meunier et al. 2009) and 0.31 μL/mL (Datta et al. 2008), respectively, assuming a flow rate of 3.0 mL/min. The actual concentration was expected to vary somewhat as a function of flow through the occluded artery because of the changing size and shape of the clot. The concentration of infused rt-PA was a thousand-fold higher than the endogenous t-PA concentration. Datta et al. (2008) demonstrated negligible enhancement of lysis without the inclusion of rt-PA. We note that this previous study used 10 bolus injections of Definity rather than a continuous infusion scheme with intermittent ultrasound used here and described next. Nonetheless, the treatment combination of plasma, Definity and ultrasound exposure was not tested in this experiment.

Cavitation detection

The *ex vivo* artery within its holder was vertically mounted in a tank filled with 37°C purified (0.2 micron filter, Memtrex, Trevose, PA, USA) and degassed (1.65 ± 0.3 mg O_2/L; FiberFlo, Skippack, PA, USA) water and connected to the flow system, as shown in Figure 1. A vertical orientation was chosen to minimize bubble trapping. The artery was placed so that the upstream face of the clot was positioned at the Rayleigh distance (10.4 cm) of the 120-kHz source transducer using a three-axis translation stage (Newport 423, Irvine, CA, USA). The wall of the tank opposite the 120-kHz transducer was lined with acoustically absorbent rubber (Aptflex F48, Precision Acoustics, Dorchester, UK) to minimize acoustic reflections. A 19-mm-diameter circular single-element, unfocused 2.25-MHz transducer (Picker Roentgen GmbH, Espelkamp, Germany), which provided passive cavitation detection, was aligned confocally with the 120-kHz source transducer at an axial distance of 5.4 cm from the artery.

Ultraharmonics of the fundamental frequency are associated with stable cavitation (Ilyichev 1989; Phelps and Leighton 1997). In this experiment, ultraharmonic acoustic emissions were

the frequency components of the received signal that occurred at odd multiples of one-half the 120-kHz driving frequency (*e.g.*, 180 kHz, 300 kHz, 420 kHz, *etc*.). Cavitation signals were analyzed by sampling the amplified signal from the 2.25-MHz transducer at a rate of 25 MHz and recording 20-ms-long traces in binary format three times per second. The binary files were processed in MATLAB (The MathWorks Inc., Natick, MA, USA) to obtain power spectra. Two power spectra detected from two arteries containing static degassed saline were transformed into the frequency domain, averaged and subtracted from each experimental spectrum to reduce noise before analysis. The broadband contributions associated with inertial cavitation (Cramer and Lauterborn 1982) were subtracted from the noise-reduced spectra. The portion of the power spectra attributed to inertial cavitation was defined to be 800-Hz wide frequency bands centered ± 15 kHz from a corresponding ultraharmonic, as shown in Figure 2. The remaining ultraharmonic peaks (each with a bandwidth of 800 Hz) in the power spectrum between 300 kHz and 3.78 MHz, also shown in Figure 2, were summed. The summed ultraharmonic spectra were temporally averaged once per second to determine the total ultraharmonic energy in the acoustic cavitation emissions. The broadband energy was likewise calculated by summing the power in the bands adjacent to the ultraharmonic bands and temporally averaging once per second, then summing over the treatment period. The broadband energy was used as an indicator of inertial cavitation activity.

Before the commencement of treatment trials, conditions for optimization of maximal stable cavitation (highest sustained ultraharmonic energy) were identified in a series of experiments. Two parameters were optimized—the insonation pressure amplitude and the optimal duration of ultrasound based on the longevity and amplitude of ultraharmonic energy using Definity as a source of nuclei with a fixed ultrasound off-time to allow fresh nuclei to flow into the artery. The optimization experiments were performed in three different arteries perfused with oxygenated plasma and Definity at 0.31 μL per mL of plasma with flow rates of 1.0 and 5.0 mL/minute. The flow rates were selected to bracket the anticipated range of flow rates through the artery during thrombolysis experiments. Continuous wave ultrasound was applied for 70 s and the ultraharmonic emissions were recorded for 14 trials over a range of peak-to-peak pressure amplitudes (0.08 to 0.52 MPa). The 14 trials were performed three times in each of three arteries. The resulting emissions were analyzed as described before to determine the ultraharmonic and broadband emission energies as a function of time within each 70-s trial (total $n = 126$).

Once initiated, both the broadband and ultraharmonic emission powers decayed with time. The broadband power typically decayed within 2 s and lasted longer in duration for higher-pressure amplitudes. The ultraharmonic power decayed more slowly and lasted the longest for pressures around 0.44 MPa. Because the cavitation emission powers decayed with time, it was determined that the optimal ultrasound insonation pattern would require quiescent periods to allow a fresh infusion of Definity and plasma to fill the vessel. The optimal duration of the quiescent period depended on the flow rate and artery diameter. A combination of the slowest flow rate (1.0 mL/min) and largest vessel (6-mm inner diameter) was used to determine a worst-case required quiescent period of 19.5 s.

Then for each of the $n = 9$ trials, using their respective instantaneous ultraharmonic energy function and the fixed values of a 30-min treatment period and a 19.5-s ultrasound quiescent period between insonations, the pressure amplitude and on-time that maximized the cumulative ultraharmonic energy per treatment period were determined. Using a subset of the data generated in the stable cavitation optimization experiment, the total ultraharmonic emission energy was calculated for a simulated 30-min treatment period for a range of continuous wave (CW) ultrasound on-times, using a fixed quiescent period of 19.5 s. Only pressure amplitudes yielding consistent stable cavitation were used for the simulation (0.37, 0.41, 0.44 and 0.52 MPa, $n = 36$). Shown in Figure 3 is a representative plot of normalized ultraharmonic energy as a function of interval duration of the CW ultrasound. An insonation pressure amplitude of 0.44 MPa and a CW ultrasound interval duration of 8.5 s yielded the maximum ultraharmonic emissions over the simulated 30-min treatment period.

Artery handling

Arteries were prepared and aligned within the confocal region of the 120-kHz transducer and 2.25-MHz passive cavitation detector. The cable to the 120-kHz transducer was simply disconnected for those arteries that were not slated to receive insonation. At the commencement of each trial, the syringe pump was turned on to infuse the therapeutic (or oxygenated plasma if no therapeutic was indicated), and after a quick verification of flow using a clinical ultrasound scanner at a mechanical index of 0.06 (Philips HDI 5000 with C5-2 curved array, Royal Philips Electronics NV, Amsterdam, The Netherlands), the 120-kHz intermittent ultrasound was energized (0.44 MPa peak-to-peak pressure amplitude, 8.5-s interval duration, 19.5-s quiescent period) and the trial commenced. After treatment or sham treatment, each artery with clot was removed, blotted and weighed. To allow co-location of clot and artery in the histology detailed next, the clot was not removed post treatment, and the mass loss was calculated using pretreatment weights of the artery and clot. The artery with clot was sliced in approximately 4-mm-thick cross sections, and one segment was preserved in formalin and the remaining segments were frozen in Tissue-Tek Optimal Cutting Temperature compound (Ted Pella Inc., Redding, CA, USA), and stored at −80°C.

Clot mass loss analysis

Differences in clot mass loss between experimental groups were examined using a two-way analysis of variance (ANOVA) with repeated measures. The two independent variables considered were presence or absence of ultrasound, and presence or absence of the mixture of rt-PA and Definity. A p-value ≤ 0.05 (two-tailed) was considered statistically significant.

Clot particle analysis

The concentration and size distribution of clot fragments in the effluent were measured and compared with those of naïve pooled porcine plasma. The effluent over each 30-min treatment was collected in separate vials preloaded with 400 mg of aminocaproic acid (ACA), a plasminogen-activator inhibitor, to halt the activity of rt-PA immediately after exiting the flow model. The final concentration of ACA was 8–160 mg/mL and did not alter the pH of the effluent (7.37 ± 0.03). A Z1 Series Coulter Counter (Beckman Coulter, Inc.,

Brea, CA, USA) with a 100-μm aperture was used to measure the number density of particles in 800-μL aliquots of the effluent in three size bins: 2–4 μm, 4–10 μm and 10–40 μm. The particle number density was multiplied by the total effluent volume in the 30-min treatment period to estimate total particle count in each size bin. The software used by the Coulter Counter to account for particle coincidence caused by large particle counts in the 2–4-μm size bin prevented measurements of particle number density above 40 μm. To reveal the presence of any particles larger than 40 μm, light microscopy of the effluent samples was performed. A 200-μL aliquot of each sample was pipetted onto a microscope slide and analyzed with an Olympus IX71 inverting light microscope (Olympus America Inc., Center Valley, PA, USA; 40x objective). Bright-light images were acquired of the largest clot fragments containing erythrocyte aggregations on each slide by an individual blinded to experimental treatments.

Tissue histology

Each arterial segment was cut into 5-micron-thick sections and mounted on glass slides. Formalin-preserved sections were stained with hematoxylin and eosin for routine histologic evaluation. These were examined by a clinical pathologist, blinded to treatment type, using an Olympus BX61 microscope equipped with a Retiga 2000R FAST 1394 FireWire monochrome 12-bitcooled digital camera (Olympus America, Center Valley, PA, USA) to assess for tissue damage. A correlation coefficient was calculated for the degree of endothelial loss and penetration of rt-PA into the arterial wall. Frozen sections were immunostained using polyclonal goat anti-human-t-PA immunoglobulin (American Diagnostics Inc., Stamford, CT, USA). A representative set of fluorescence micrographs from each artery was assessed by two individuals blinded to the ultrasound exposure conditions using a program written in MATLAB that allowed the user to subtract the autofluorescence of the tissues and determine the remaining area of tissue demonstrating enhanced fluorescence. This fluorescent area was normalized to the total artery or clot cross-sectional area, as appropriate. Because of difficulties in tissue preservation, the sample sizes for tissue histology were four in the plasma treatment group, four for plasma and rt-PA, five for rt-PA and Definity, six for plasma and ultrasound, five for plasma with rt-PA and ultrasound and five for plasma with rt-PA plus ultrasound and Definity. The goal was to determine whether rt-PA penetrated preferentially into a specific region of the residual clot, and whether rt-PA penetrated into the arterial wall. ANOVA with an α of 0.05 and follow-up Student's *t*-tests were performed to assess the relationship between treatment and fluorescent enhancement in both clots and arteries.

RESULTS

Cavitation emissions

As shown in Figure 4, the total ultraharmonic energy within the simulated treatment period, corresponding to the presence of stable cavitation, was dependent on the presence of both Definity and 120-kHz intermittent ultrasound. At a peak-to-peak pressure amplitude of 0.44 MPA, oxygenated porcine plasma provided a poor substrate for stable cavitation, whereas in the presence of Definity, the clot-filled arteries were exposed to robust stable cavitation. The amount of total broadband energy was 22 dB less than the amount of ultraharmonic energy

for the treatment including both Definity and intermittent ultrasound. The mean duration of stable and inertial cavitation for the combined rt-PA, Definity and intermittent ultrasound within a 30-min treatment period was 510 ± 79 s and 190 ± 178 s, respectively. The overall ultrasound "on-time" was 567 s. Thus, stable and inertial cavitation were present for approximately 90% and 34% of the ultrasound "on-time," respectively.

Recanalization of artery with clot lysis

The flow through the *ex vivo* system varied over the course of each thrombolysis trial. The mean flow rate across all trials was 2.2 ± 1.5 mL/min with a range of 0–7.8 mL/min. However, the mean flow rate was not statistically different among treatment groups. It was noted that the intra-arterial flow seated the clot against the downstream cannula during the entire treatment period in all of the trials, thus maintaining flow restriction.

On the basis of the measured volumetric flow rates, the concentration of rt-PA in the treated arteries was calculated to be 7.1 ± 3.8 μg/mL. Shaw et al. (2008) have demonstrated lytic efficacy over this concentration range. Likewise, the concentration of Definity in the treated arteries was calculated to be 0.79 ± 0.47 μL/mL. Treatment arms did not have statistically significantly different rt-PA or Definity concentrations ($p > 0.1$) as determined by two-way ANOVA.

Clot mass loss

Shown in Figure 5 are the mean clot mass losses for each treatment. A two-way ANOVA with repeated measures revealed that there are significant differences in mass loss among arteries perfused with rt-PA and Definity and those perfused with plasma alone, with and without ultrasound, F (5, 32) = 63.2, $p < 0.0001$. The ANOVA further showed that effects of rt-PA with Definity do interact significantly with the effects of ultrasound. This phenomenon was studied further with four paired t-tests (two-tailed). To keep the overall level of significance at 0.05, each individual t-test needed to be performed with an alpha of 0.0125 (0.05/4) to be considered significant. With ultrasound, there was a significant difference between groups with and without rt-PA and Definity ($p < 0.0001$). For those arteries perfused with a combination of rt-PA and Definity, there was a significant difference between those clots exposed to ultrasound and those that were not exposed ($p < 0.0001$). In the absence of ultrasound, treatment with rt-PA and Definity produced a significantly higher mass loss than treatment with plasma alone ($p = 0.0001$). With no rt-PA or Definity present, however, the effect of ultrasound was not significant ($p = 0.19$). A follow-up Student's t-test showed no difference between rt-PA–treated clots with or without Definity.

Clot particle analysis

The data collected from the Coulter Counter and microscope images were used to assess two characteristics of the effluent particles: (i) the total number of particles (particle number density times total volume collected) in three size bins: 2–4 μm, 4–10 μm and 10–40 μm; and (ii) the largest particles remaining after each treatment. Table 2 shows the mean total number of particles in the three size bins collected downstream for each treatment protocol over 30 min. In addition, the same size distribution data is given for naïve porcine plasma. A

one-way unbalanced ANOVA showed that there was no significant difference between the mean particle counts in naïve *vs*. control plasma in the 2–4-μm (F (1, 8) = 2.4, p = 0.16) and 10–40-μm size bins (F (1, 8) = 5.2, p = 0.06). However, there was a significantly higher number of particles in the 4–10-μm-size range in the control treated clots, F (1, 8) = 6.7, p = 0.037. There was also no significant difference between the mean particle counts in any of the size bins between any treatment groups, with the exception of the 4–10-μm-size bin between the control and ultrasound treatments, F (5, 32) = 25.3, p = 0.002.

The microscope images revealed a sparse number of particles in the 40–80-μm-size range, but did not reveal any particles >80 μm in diameter. A one-way unbalanced ANOVA showed that there was no correlation between the size of the largest particle in each image and treatment group, F (5, 32) = 0.9, p = 0.51. Figure 6 shows an example of a bright-field, light microscope image of fragments from clots exposed to 120-kHz ultrasound, rt-PA and Definity.

Tissue histology

Pathologic examination of hematoxylin and eosin–stained, formalin-preserved artery slices revealed that all arteries had undergone some degree of endothelial damage. A fairly large percent of the lumen perimeters, 64% ± 28%, demonstrated some degree of endothelial cell distress or loss. Four arteries had <20% endothelial survival. ANOVA testing showed that no difference in endothelial damage among treatment groups could be statistically demonstrated, F (5, 22) = 1.57, p = 0.21. Endothelial loss was not a function of mean flow during the 30-min treatment period. ANOVA testing did not demonstrate a difference among arteries treated on the day of harvest, one day later or two days later, F (2, 25) = 1.24, p = 0.31. A variable portion of each arterial endothelium was obscured by the close proximity of the luminal blood clot, but the remaining perimeter was analyzed except in five arteries, distributed among treatment groups, in which the entire endothelium was obscured. The tunica media of the arteries appeared largely unaffected, although early hydropic changes were apparent in the superficial medial layers of approximately 10% of the vessels, distributed among treatment groups, as illustrated in Figure 7. The tunica adventitia was apparently unaffected.

Image analysis, performed by two observers blinded to experimental conditions, of the clot-artery slices that had been stained with anti–t-PA antibody revealed no difference among treatment groups in the binding of the antibody within the clot or within the wall of the arteries, by ANOVA testing (F (5, 29) = 1.5, p = 0.21 for clots; F (5, 30) = 0.51, p = 0.76 for arteries). The degree of binding also showed no correlation with the degree of endothelial loss (r = 0.9, p = 0.3). All arteries showed a slight enhancement of both the clot and the arterial wall, as shown in Figure 8. This effect was more pronounced in some individual specimens than in others, but the pronouncement was equally distributed among treatment groups, including those receiving no exogenous t-PA. A slight enhancement of the periphery of each clot was visible as shown in Figure 8.

DISCUSSION

This study examined the effect of cavitation driven by 120-kHz ultrasound on rt-PA lysis of whole blood clots in an *ex vivo* artery with physiologic flow. As observed in an *in vitro* porcine clot model in static plasma, clots exposed to rt-PA over 30 min exhibited a higher mass loss than those clots exposed to plasma alone (Holland et al. 2008). Porcine clots exposed to rt-PA and plasma in the *ex vivo* artery model showed a mean mass loss of 29% and porcine clots exposed to the same concentration of rt-PA in static plasma had a lower mean mass loss of 12.5%, likely because flow replenishes the concentration of rt-PA and plasminogen at the clot boundary and promotes mixing (Fig. 5). Also, clots exposed to serial infusions of Definity, rt-PA and 120-kHz pulsed ultrasound (80% duty cycle) had a 26.3% clot mass loss (Datta et al. 2008) and a twofold increase over rt-PA alone. Similarly, clots in the arterial model exposed to Definity, rt-PA and intermittent ultrasound exhibited a 83% mean clot mass loss, which is almost a threefold increase over rt-PA alone. Note that the length of the clots within the *ex vivo* artery exceeded the −3-dB beam width of the 120-kHz source transducer. Therefore, a portion of the clot would not be expected to exhibit enhanced thrombolysis, limiting the total thrombolytic efficacy to less than 100%. Future studies should be aimed at comparing the thrombolytic efficacy of intermittent continuous wave ultrasound vs. pulsed ultrasound in the presence of flow.

Other studies (Mizushige et al. 1999; Nedelmann et al. 2002; Cintas et al. 2004; Unger et al. 2005; Molina et al. 2006; Porter et al. 2006) support the observation that a combination of a thrombolytic agent, an echo contrast agent and ultrasound can result in increased clot mass loss. *In vitro* experiments by Datta et al. (2008) revealed that stable cavitation was responsible for the enhancement. In the present study, exposure to stable cavitation was maximized through careful selection of ultrasound parameters and continuous infusion of a nucleation agent, and correlated highly with a substantial increase in clot mass loss (Fig. 5). The acoustic pressure that promoted stable cavitation also produced some inertial cavitation, and no effort was made here to differentiate between the separate effects of the two cavitation modes (Fig. 4). However, it should be noted that the ultraharmonic energy was 22 dB higher than the broadband energy in those clots exposed to rt-PA, Definity and intermittent ultrasound. In future studies, a higher acoustic pressure amplitude that maximizes inertial cavitation could be included to elucidate the enhancement of rt-PA thrombolysis caused by inertial cavitation, and to explore potential endothelial bioeffects. No experiments were performed attempting to maximize inertial cavitation; this would be an interesting treatment for future studies. Intermittent ultrasound and rt-PA exposure without the nucleation agent (Definity), produced negligible stable cavitation (Fig. 4). This lack of cavitation nucleation was also observed by Datta et al. (2008) in static rt-PA and plasma exposed to pulsed 120-kHz ultrasound.

Even in the very-low-flow environment of this partially occlusive clot model, the moving fluid both delivers and carries away therapeutics and fibrin degradation products, dramatically changing the drug delivery setting compared with models in which flow is not present (Jadhav et al. 2007). In this study, the delivery rate, or flow rate, of cavitation nuclei in the form of Definity into the treatment region was the determining factor in the choice of intermittent ultrasound as opposed to pulsed ultrasound for maximization of stable

cavitation. This observation revealed that the selection of a quiescent ultrasound period to permit the influx of artificial cavitation nuclei is an essential parameter in the design of an ultrasound-enhanced rt-PA thrombolysis treatment.

The advantages of the *ex vivo* system in the study of sonothrombolysis lie in the combination of a cavitational milieu resembling that *in vivo* with minimization of attenuation of the cavitation signal that greatly complicates studies in living, whole animals (Holland et al. 1996). Furthermore, the presence of living tissue can provide information about vascular bioeffects. This *ex vivo* model is a useful intermediate between *in vitro* and *in vivo* experiments to help harness the mechanism of thrombolytic enhancement in a carefully controlled environment.

Arteries in all treatment groups experienced loss of endothelium, an expected effect on this delicate tissue in a low-perfusion environment with limited oxygen (Ogawa et al. 1990). In this work, the stress of excision and refrigerated storage no doubt contributed to the susceptibility of endothelium to this insult (Zilla et al. 1993), but endothelial damage in an ischemic environment is a well known phenomenon. Gerriets et al. (2009) observed penetration of Evans blue dye across the cerebral endothelium of rats in an ischemic stroke model as early as 20 min after middle cerebral artery occlusion, denoting endothelial damage. These investigators also noted vasogenic cerebral edema in their model. Likewise, a small percentage of vessels in our study (10%) exhibited edema of the tunica media (Fig. 7). Nakano et al. (2006) noted the passage of intravascular computed tomography contrast material across the blood-brain barrier in humans within 20 min after the onset of ischemic stroke, without observable hemorrhage. Thus vascular ischemia is associated with a limited leaky endothelium (Dauber et al. 1985, 1990; Menon et al. 2004).

Increased t-PA and rt-PA penetration into the arterial tissue was not observed in arteries exposed to 120-kHz ultrasound. It is unknown whether the large size of the t-PA protein (Rijken et al. 1979; Rånby et al. 1982) or some other factor prevented its consistent migration into the arterial wall, even in cases where a significant portion of the endothelium was missing. Because acoustic microstreaming, thought to be one possible intermediate mechanism of cavitation-enhanced drug delivery (Hitchcock et al. 2010), is highly localized to the region immediately surrounding the bubble, it may be that a lack of targeting of rt-PA to the endothelium or other arterial tissues may limit movement of the protein into the arterial wall in significant quantities.

The consistent distribution of rt-PA throughout the clot shown in Figure 8 may be attributable to flow through the clot, a scenario proposed by Roberts (1974). Because the rt-PA is self-targeting to fibrin (Siddiqi et al. 1998), the pattern of enhancement of rt-PA in the clot would be expected to conform to the geometry of the fibrin mesh. In the images analyzed here, that mesh took up a relatively small portion of each image, the remainder consisting of the heavy density of red blood cells in these whole blood clots, and thus the overall fluorescence of the clots, as shown in Figure 8, was moderate.

The sizes of the major cerebral arteries, as cited by microanatomy studies (Gomes et al. 1986; Smoker et al. 1986; Russell et al. 1991; Ohki et al. 1998; Pai et al. 2005; Conijn et al.

2009) range from 0.83–7.5 mm in diameter. The middle cerebral artery, a primary location for thrombus occlusion, has a mean diameter of 2.4 mm (Russell et al. 1991; Pai et al. 2005). The smallest cerebral artery perforators are those of the posterior cerebral artery, with a mean diameter of 146 μm (Marinkovic et al. 1990). Clot fragments in the effluent were well below this size range, as confirmed by the microscope images. The increased number of particles in the 4–10-μm size range between naïve and control-treated plasma is likely a result of erythrocytes dislodged from the clot in the *ex vivo* artery model. Furthermore, these larger particles were not seen in appreciable numbers. Together, these data suggest that ultrasound exposure, which produces stable cavitation nucleated from Definity, does not exacerbate the production of large clot fragments.

The limitations of the *ex vivo* model include the lack of whole blood flow; endocrine, sympathetic and parasympathetic signaling to the artery; and shifts in homeostatic variables (blood pH, oxygenation, temperature, *etc*.) that might occur in response to stroke *in vivo*. In addition, the use of porcine clots may cause the clot mass loss results of this study to be artificially low. Porcine clots are known to be especially resistant to thrombolysis (Flight et al. 2006). Specific factors for this resistance include low concentrations of plasminogen in porcine blood or plasma (Holland et al. 2008) and a high concentration of plasminogen activator inhibitor 1, which is more active than the human form (Fay et al. 1996).

Further studies are needed to understand the optimization of contrast medium concentration, ultrasound quiescent period, ultrasound pulse parameters and other variables on the stable cavitation enhancement of rt-PA thrombolysis. It should be noted that the ultrasound parameters used in this study optimized stable cavitation energy for a fixed quiescent period. This particular intermittent ultrasound scheme, although effective, has not necessarily optimized clot mass loss. In the future, low mechanical index imaging could be used to verify the presence of cavitation nuclei and thus allow adaptive quiescent periods throughout a treatment. Additional work is also needed to assay the bioeffects, and whole animal studies are a necessary next step to this end.

CONCLUSIONS

This work demonstrates significant 120-kHz ultrasound enhancement of thrombolysis of whole porcine blood clots in the presence of flowing porcine plasma. Maximization of stable cavitation in plasma flowing through *ex vivo* carotid arteries resulted from use of intermittent ultrasound with constant infusion of Definity. Arteries demonstrated endothelial damage in the low-oxygen environment of the *ex vivo* artery obstructed by a clot, but ultrasound-enhanced thrombolysis did not affect the frequency of this damage. Future use of this *ex vivo* model will enable optimization of sonothrombolysis in an *in vivo*–like environment.

Acknowledgments

The authors would like to thank Stehlin’s Meats, Cincinnati, OH, and Kaiser’s Meats, Cedar Grove, IN, for allowing time-critical tissue collection immediately after slaughter and for their skill in excision. This work was supported by the National Institutes of Health, grant numbers R01-NS047603 and T32GM063483; the University of Cincinnati Neuroscience Institute; the Albert J. Ryan Foundation Fellowship; and the Rindsberg Memorial Fellowship.

References

Akiyama M, Ishibashi T, Yamada T, Furuhata H. Low-frequency ultrasound penetrates the cranium and enhances thrombolysis in vitro. Neurosurgery. 1998; 43:828–832. [PubMed: 9766310]

Alexandrov AV. Ultrasound identification and lysis of clots. Stroke. 2004; 35:2722–2725. [PubMed: 15375301]

Baron C, Aubry JF, Tanter M, Meairs S, Fink M. Simulation of intracranial acoustic fields in clinical trials of sonothrombolysis. Ultrasound Med Biol. 2009; 35:1148–1158. [PubMed: 19394756]

Behrens S, Daffertshofer M, Spiegel D, Hennerici M. Low-frequency, low-intensity ultrasound accelerates thrombolysis through the skull. Ultrasound Med Biol. 1999; 25:269–273. [PubMed: 10320316]

Blinc A, Francis CW, Trudnowski JL, Carstensen EL. Characterization of ultrasound-potentiated fibrinolysis in vitro. Blood. 1993; 81:2636–2643. [PubMed: 8490172]

Boulaftali Y, Ho-Tin-Noe B, Pena A, Loyau S, Venisse L, Francois D, Richard B, Arocas V, Collet JP, Jandrot-Perrus M, Bouton MC. Platelet protease nexin-1, a serpin that strongly influences fibrinolysis and thrombolysis. Circulation. 2011; 123:1326–1334. [PubMed: 21403095]

Cannon CP. Exploring the issues of appropriate dosing in the treatment of acute myocardial infarction: Potential benefits of bolus fibrinolytic agents. Am Heart J. 2000; 140:S154–S160. [PubMed: 11100010]

Cintas P, Nguyen F, Boneu B, Larrue V. Enhancement of enzymatic fibrinolysis with 2-MHz ultrasound and microbubbles. J Thromb Haemost. 2004; 2:1163–1166. [PubMed: 15219200]

Conijn M, Hendrikse J, Zwanenburg J, Takahara T, Geerlings M, Mali W, Luijten P. Perforating arteries originating from the posterior communicating artery: A 7.0-Tesla MRI study. Eur Radiol. 2009; 19:2986–2992. [PubMed: 19533146]

Cramer E, Lauterborn W. Acoustic cavitation noise spectra. Appl Sci Res. 1982; 38:209–214.

Daffertshofer M, Gass A, Ringleb P, Sitzer M, Sliwka U, Els T, Sedlaczek O, Koroshetz WJ, Hennerici MG. Transcranial low-frequency ultrasound-mediated thrombolysis in brain ischemia: Increased risk of hemorrhage with combined ultrasound and tissue plasminogen activator—Results of a phase II clinical trial. Stroke. 2005; 36:1441–1446. [PubMed: 15947262]

Datta S, Coussios CC, Ammi AY, Mast TD, de Courten-Myers GM, Holland CK. Ultrasound-enhanced thrombolysis using Definity® as a cavitation nucleation agent. Ultrasound Med Biol. 2008; 34:1421–1433. [PubMed: 18378380]

Datta S, Coussios CC, McAdory LE, Tan J, Porter T, De Courten-Myers G, Holland CK. Correlation of cavitation with ultrasound enhancement of thrombolysis. Ultrasound Med Biol. 2006; 32:1257–167. [PubMed: 16875959]

Dauber IM, Pluss WT, VanGrondelle A. Specificity and sensitivity of noninvasive measurement of pulmonary vascular protein leak. J Appl Physiol. 1985; 59:564–574. [PubMed: 3928588]

Dauber IM, VanBenthuysen KM, McMurtry IF, Wheeler GS, Lesnefsky EJ, Horwitz LD, Weil JV. Functional coronary microvascular injury evident as increased permeability due to brief ischemia and reperfusion. Circ Res. 1990; 66:986–998. [PubMed: 2180590]

Fay WP, Murphy JG, Owen WG. High concentrations of active plasminogen activator inhibitor-1 in porcine coronary artery thrombi. Arterioscler Thromb Vasc Biol. 1996; 16:1277–1284. [PubMed: 8857925]

Flight SM, Masci PP, Lavin MF, Gaffney PJ. Resistance of porcine blood clots to lysis relates to poor activation of porcine plasminogen by tissue plasminogen activator. Blood Coagul Fibrinolysis. 2006; 17:417–420. [PubMed: 16788320]

Francis CW, Blinc A, Lee S, Cox C. Ultrasound accelerates transport of recombinant tissue plasminogen activator into clots. Ultrasound Med Biol. 1995; 21:419–424. [PubMed: 7645133]

Francis CW, Onundarson PT, Carstensen EL, Blinc A, Meltzer RS, Schwarz K, Marder VJ. Enhancement of fibrinolysis in vitro by ultrasound. J Clin Invest. 1992; 90:2063–2068. [PubMed: 1430229]

Gerriets T, Walberer M, Ritschel N, Tschernatsch M, Mueller C, Bachmann G, Schoenburg M, Kaps M, Nedelmann M. Edema formation in the hyperacute phase of ischemic stroke: Laboratory investigation. J Neurosurg. 2009; 111:1036–1042. [PubMed: 19408985]

Gomes FB, Dujovny M, Umansky F, Berman SK, Diaz FG, Ausman JI, Mirchandani GG, Ray WJ. Microanatomy of the anterior cerebral artery. Surg Neurol. 1986; 26:129–141. [PubMed: 3726739]

Hitchcock KE, Caudell DN, Sutton JT, Klegerman ME, Vela D, Pyne-Geithman GJ, Abruzzo T, Cyr PE, Geng YJ, McPherson DD, Holland CK. Ultrasound-enhanced delivery of targeted echogenic liposomes in a novel ex vivo mouse aorta model. J Control Release. 2010; 144:288–295. [PubMed: 20202474]

Holland CK, Deng CX, Apfel RE, Alderman JL, Fernandez LA, Taylor KJW. Direct evidence of cavitation in vivo from diagnostic ultrasound. Ultrasound Med Biol. 1996; 22:917–925. [PubMed: 8923710]

Holland CK, Vaidya SS, Coussios CC, Shaw GJ. Thrombolytic effects of 120-kHz and 1-MHz ultrasound and tissue plasminogen activator on porcine whole blood clots. J Acoust Soc Am. 2002; 112:2370.

Holland CK, Vaidya SS, Datta S, Coussios CC, Shaw GJ. Ultrasound-enhanced tissue plasminogen activator thrombolysis in an in vitro porcine clot model. Thromb Res. 2008; 121:663–673. [PubMed: 17854867]

Ilyichev V. Spectral characteristics of acoustic cavitation. Ultrasonics. 1989; 27:357–361. [PubMed: 2815406]

Jadhav S, Eggleton CD, Konstantopoulos K. Mathematical modeling of cell adhesion in shear flow: Application to targeted drug delivery in inflammation and cancer metastasis. Curr Pharm Design. 2007; 13:1511–1526.

Jern C, Seeman-Lodding H, Biber B, Winso O, Jern S. An experimental multiple-organ model for the study of regional net release/uptake rates of tissue-type plasminogen activator in the intact pig. Thromb Haemost. 1997; 78:1150–1156. [PubMed: 9308769]

Kehr J, Yoshitake T, Wang FH, Wynick D, Holmberg K, Lendahl U, Bartfai T, Yamaguchi M, Hokfelt T, Ogren SO. Microdialysis in freely moving mice: Determination of acetylcholine, serotonin and noradrenaline release in galanin transgenic mice. J Neurosci Methods. 2001; 109:71–80. [PubMed: 11489302]

Li C, Engstrom G, Hedblad B, Berglund G, Janzon L. Risk factors for stroke in subjects with normal blood pressure: A prospective cohort study. Stroke. 2005; 36:234–238. [PubMed: 15618439]

Marcu CB, Kramer C, Donohue TJ. Giant left atrial thrombus successfully treated with anticoagulation. Heart Lung Circ. 2007; 16:55–56. [PubMed: 17045526]

Marinkovic S, Milisavljevic M, Marinkovic Z. Anastomoses among the perforating arteries of the brain. Microanatomy and clinical significance. Neurologija. 1990; 39:107–114. [PubMed: 2267048]

Menon DK, Coles JP, Gupta AK, Fryer TD, Smielewski P, Chatfield DA, Aigbirhio F, Skepper JN, Minhas PS, Hutchinson PJ, Carpenter TA, Clark JC, Pickard JD. Diffusion limited oxygen delivery following head injury. Crit Care Med. 2004; 32:1384–1390. [PubMed: 15187523]

Meunier JM, Holland CK, Pancioli AM, Lindsell CJ, Shaw GJ. Effect of low frequency ultrasound on combined rt-PA and eptifibatide thrombolysis in human clots. Thromb Res. 2009; 123:528–536. [PubMed: 18619651]

Mizushige K, Kondo I, Ohmori K, Hirao K, Matsuo H. Enhancement of ultrasound-accelerated thrombolysis by echo contrast agents: Dependence on microbubble structure. Ultrasound Med Biol. 1999; 25:1431–1437. [PubMed: 10626631]

Molina CA, Ribo M, Rubiera M, Montaner J, Santamarina E, Delgado-Mederos R, Arenillas JF, Huertas R, Purroy F, Delgado P, Alvarez-Sabín J. Microbubble administration accelerates clot lysis during continuous 2-MHz ultrasound monitoring in stroke patients treated with intravenous tissue plasminogen activator. Stroke. 2006; 37:425–429. [PubMed: 16373632]

Mueller HS, Dyer A, Greenberg MA. The thrombolysis in myocardial infarction (TIMI) trial. Phase I findings. N Engl J Med. 1985; 312:932–936. [PubMed: 4038784]

Mutch NJ, Koikkalainen JS, Fraser SR, Duthie KM, Griffin M, Mitchell J, Watson HG, Booth NA. Model thrombi formed under flow reveal the role of factor XIII-mediated cross-linking in resistance to fibrinolysis. Thromb Haemost. 2010; 8:2017–2024.

Nakano S, Iseda T, Yoneyama T, Wakisaka S. Early CT signs in patients with acute middle cerebral artery occlusion: Incidence of contrast staining and haemorrhagic transformations after intra-arterial reperfusion therapy. Clin Radiol. 2006; 61:156–162. [PubMed: 16439221]

Nedelmann M, Eicke BM, Lierke EG, Heimann A, Kempski O, Hopf HC. Low-frequency ultrasound induces nonenzymatic thrombolysis in vitro. J Ultrasound Med. 2002; 21:649–656. [PubMed: 12054301]

Ogawa S, Gerlach H, Esposito C, Pasagian-Macaulay A, Brett J, Stern D. Hypoxia modulates the barrier and coagulant function of cultured bovine endothelium. Increased monolayer permeability and induction of procoagulant properties. J Clin Invest. 1990; 85:1090–1098. [PubMed: 2156893]

Ohki T, Marin ML, Lyon RT, Berdejo GL, Soundararajan K, Ohki M, Yuan JG, Faries PL, Wain RA, Sanchez LA, Suggs WD, Veith FJ. Ex vivo human carotid artery bifurcation stenting: Correlation of lesion characteristics with embolic potential. J Vasc Surg. 1998; 27:463–471. [PubMed: 9546231]

Pai SB, Varma RG, Kulkarni RN. Microsurgical anatomy of the middle cerebral artery. Neurol India. 2005; 53:186–190. [PubMed: 16010057]

Phelps AD, Leighton TG. The subharmonic oscillations and combination-frequency subharmonic emissions from a resonant bubble: Their properties and generation mechanisms. Acustica. 1997; 83:59–66.

Pond, WG.; Mersmann, HJ. Biology of the Domestic Pig. Ithaca, NY: Comstock Publishing Associates; 2001.

Porter TM, Holland CK, Meunier JM, Shaw GJ. Enhancement of recombinant tissue-plasminogen activator (rt-PA) activity with 2-MHz transcranial Doppler ultrasound. J Acoust Soc Am. 2006; 120:3004.

Rånby M, Bergsdorf N, Nilsson Tr. Enzymatic properties of the one-and two-chain form of tissue plasminogen activator. Thromb Res. 1982; 27:175–183. [PubMed: 6890245]

Rijken DC, Wijngaards G, Zaal-de Jong M, Welbergen J. Purification and partial characterization of plasminogen activator from human uterine tissue. Biochim Biophys Acta. 1979; 580:140–153. [PubMed: 121055]

Roberts W. Rheology of fibrin clots. I. Dynamic viscoelastic properties and fluid permeation. Biophys Chem. 1974; 1:152–160. [PubMed: 4425722]

Russell D, Madden KP, Clark WM, Sandset PM, Zivin JA. Detection of arterial emboli using doppler ultrasound in rabbits. Stroke. 1991; 22:253–258. [PubMed: 2003290]

Saguchi T, Onoue H, Urashima M, Ishibashi T, Abe T, Furuhata H. Effective and safe conditions of low-frequency transcranial ultrasonic thrombolysis for acute ischemic stroke. Neurologic and histologic evaluation in a rat middle cerebral artery stroke model. Stroke. 2008; 39:1007–1011. [PubMed: 18239172]

Shaw GJ, Hahn N, Wagner KR, Holland CK. Ultrasound-assisted thrombolysis in an in-vitro clot model. Acad Emerg Med. 2001; 8:542.

Shaw GJ, Meunier JM, Lindsell CJ, Holland CK. Tissue plasminogen activator concentration dependence of 120 kHz ultrasound-enhanced thrombolysis. Ultrasound Med Biol. 2008; 34:1783–1792. [PubMed: 18468773]

Siddiqi F, Odrljin TM, Fay PJ, Cox C, Francis CW. Binding of tissue-plasminogen activator to fibrin: Effect of ultrasound. Blood. 1998; 91:2019–2025. [PubMed: 9490686]

Siegel RJ, Atar S, Fishbein MC, Brasch AV, Peterson TM, Nagai T, Pal D, Nishioka T, Chae JS, Birnbaum Y, Zanelli C, Luo H. Noninvasive, transthoracic, low-frequency ultrasound augments thrombolysis in a canine model of acute myocardial infarction. Circulation. 2000; 101:2026–2029. [PubMed: 10790341]

Smoker W, Price M, Keyes W, Corbett J, Gentry L. High-resolution computed tomography of the basilar artery: 1. Normal size and position. AJNR Am J Neuroradiol. 1986; 7:55–60. [PubMed: 3082144]

Sobbe A, Stumpff U, Truebestein G. Thrombolysis by ultrasound. Die Ultraschall Auflosung Von Thromben. 1974; 52:1117–1121.

Thorne GD, Paul RJ. Effects of organ culture on arterial gene expression and hypoxic relaxation: Role of the ryanodine receptor. Am J Physiol Cell Physiol. 2003; 284:C999–C1005. [PubMed: 12477664]

Trubestein G, Engel C, Etzel F, Sobbe A, Cremer H, Stumpff U. Thrombolysis by ultrasound. Clin Sci Mol Med Suppl. 1976; 3:697s–698s. [PubMed: 1071713]

Undas A, Brozek J, Jankowski M, Siudak Z, Szczeklik A, Jakubowski H. Plasma homocysteine affects fibrin clot permeability and resistance to lysis in human subjects. Arterioscler Thromb Vasc Biol. 2006a; 26:1397–1404. [PubMed: 16574890]

Undas A, Stepien E, Tracz W, Szczeklik A. Lipoprotein(a) as a modifier of fibrin clot permeability and susceptibility to lysis. Thromb Haemost. 2006b; 4:973–975.

Unger, E.; Matsunaga, TO.; Zutshi, R.; Labell, R.; Porter, TR.; Lof, J.; Xie, F.; Ferrara, K.; Dayton, P.; Bloch, S. Sonothrombolysis with phospholipid-coated perfluoropropane microbubbles. 4th International Symposium on Therapeutic Ultrasound AIP Conference Proceedings; 2005. p. 58-61.

Zilla P, Von Oppell U, Deutsch M. The endothelium: A key to the future. J Cardiac Surg. 1993; 8:32–60.

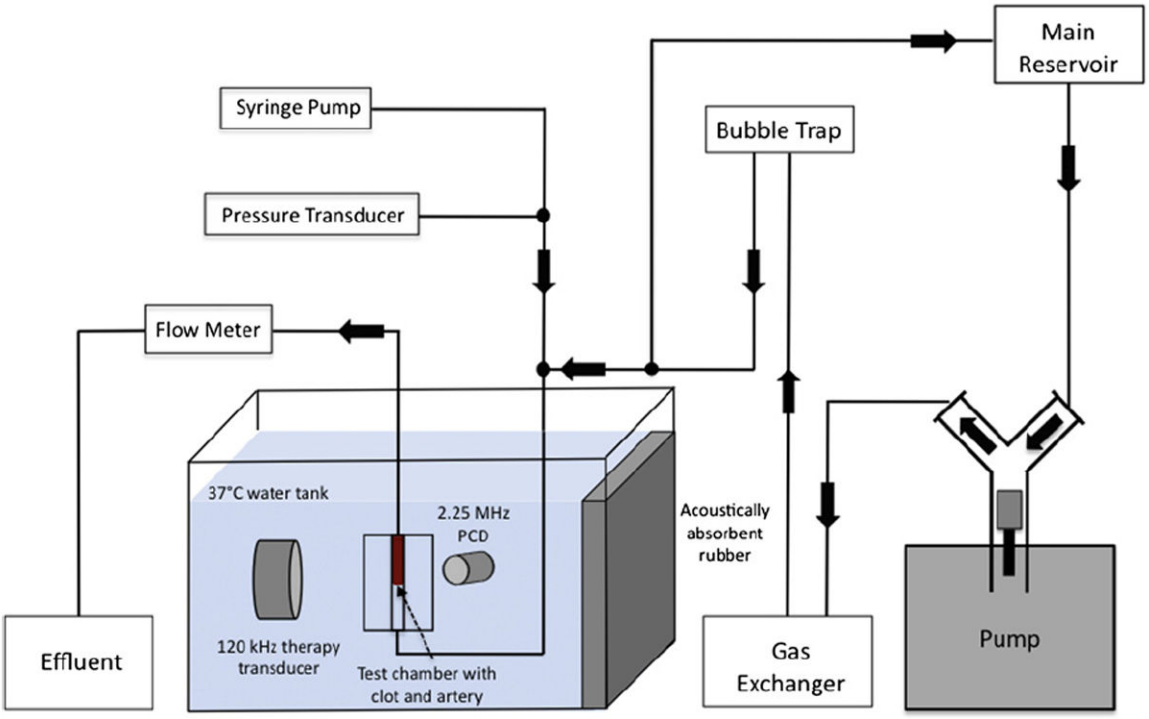

Fig. 1.

Experimental setup. The 120-kHz therapy transducer and the 2.25-MHz passive cavitation detector (PCD) are confocally aligned with the proximal edge of the clot.

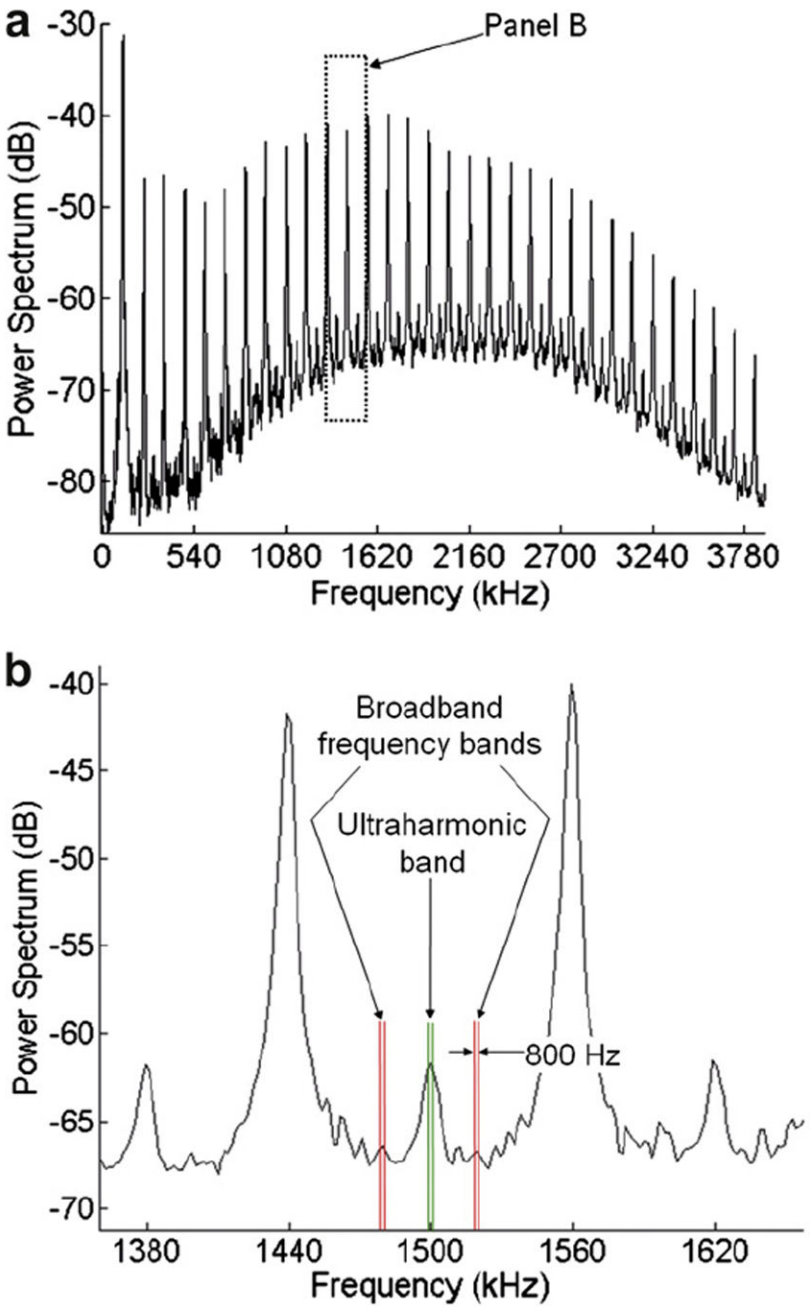

Fig. 2.

(a) A typical power spectrum for clots in arteries perfused with rt-PA and Definity in porcine plasma and insonated at a 0.44-MPa peak-to-peak pressure amplitude at 120 kHz. (b) Close-up of spectrum in (a) showing frequency bands used in the analysis of power spectra to calculate the total ultraharmonic and broadband energies. Each broadband frequency band is centered 15 kHz from the nearest ultraharmonic peak.

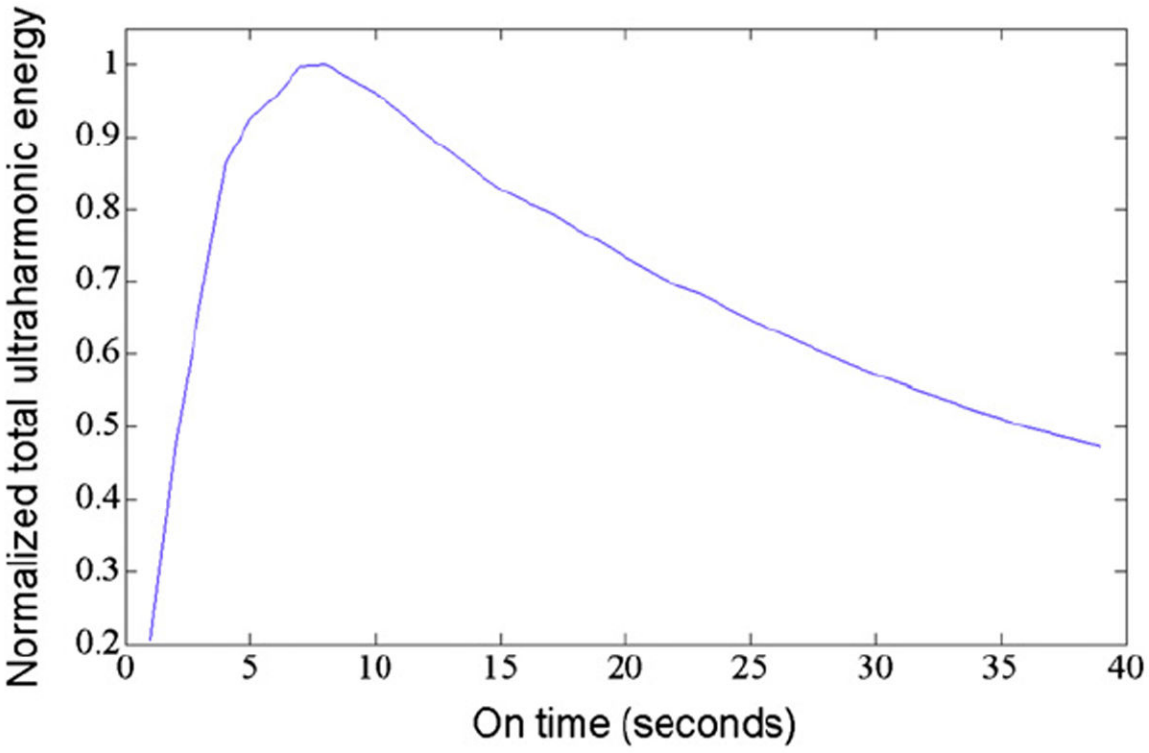

Fig. 3.

A typical plot of normalized total ultraharmonic energy as a function of on-time extrapolated over 30 min for clots in arteries perfused with rt-PA and Definity in porcine plasma and exposed to 70 s of intermittent 120-kHz ultrasound at a pressure amplitude of 0.44-MPa peak to peak.

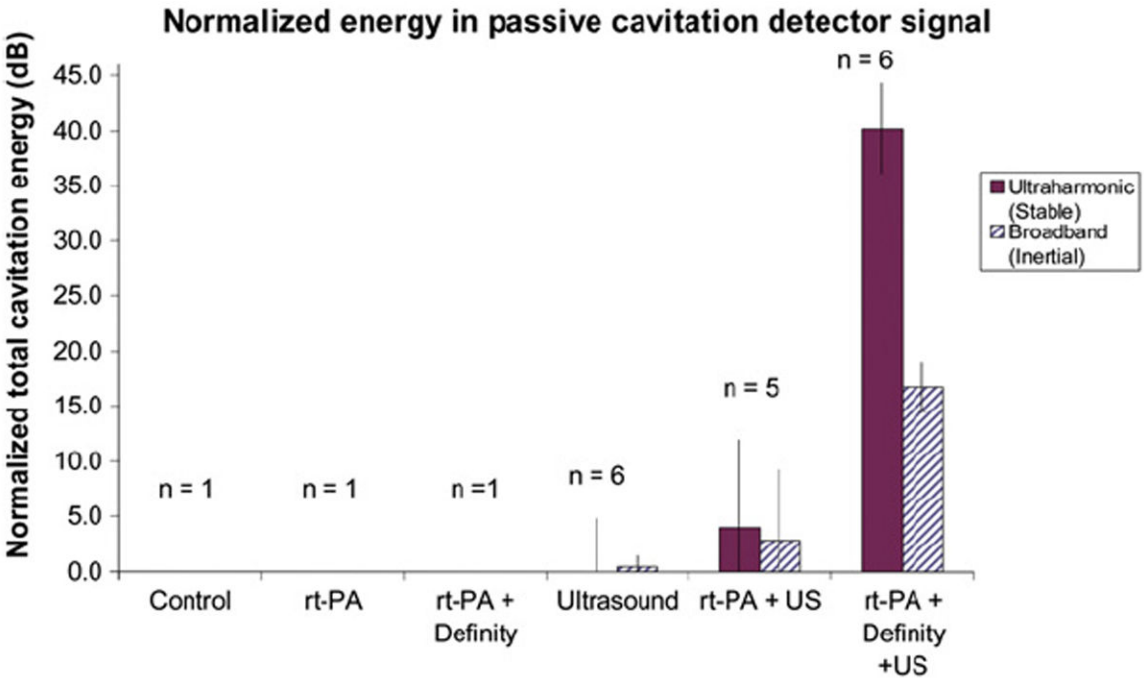

Fig. 4.

The total energy in ultraharmonic and broadband frequency bands of the passive cavitation detector signal, normalized so that the measured noise level is equal to zero. Note that the vertical scale is in decibels.

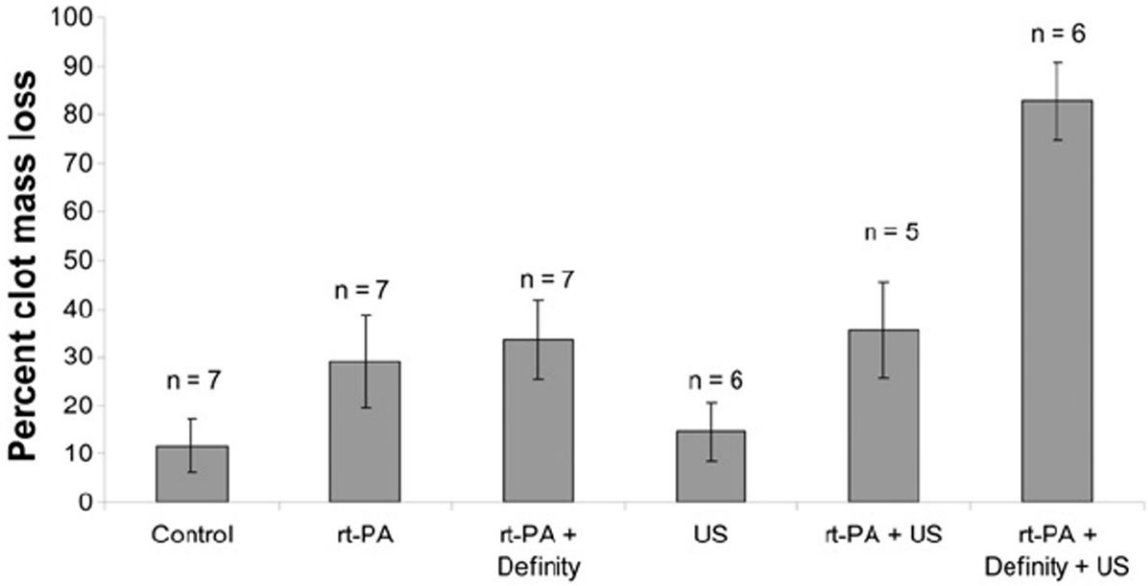

Fig. 5.

Mean percent clot mass loss by treatment group. Control clots were exposed only to flowing porcine plasma. Error bars represent one standard deviation.

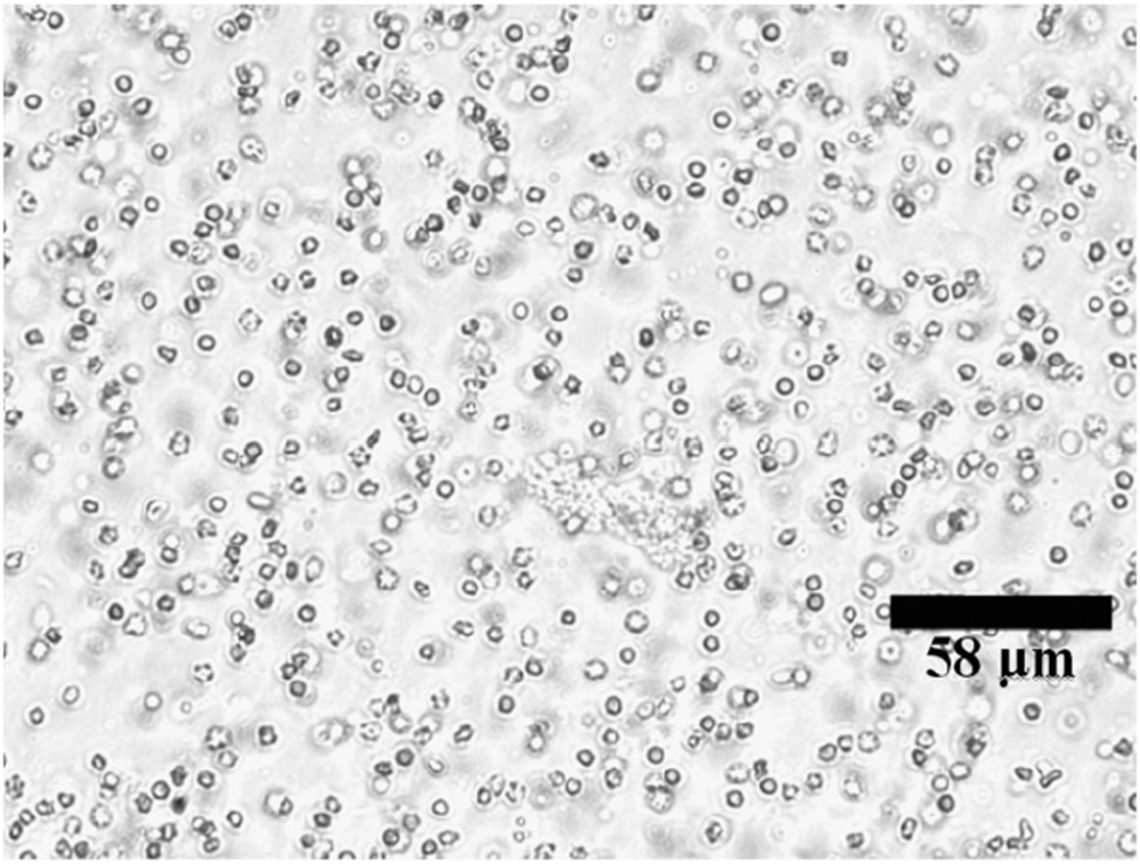

Fig. 6.
Representative micrograph of clot lysis fragments.

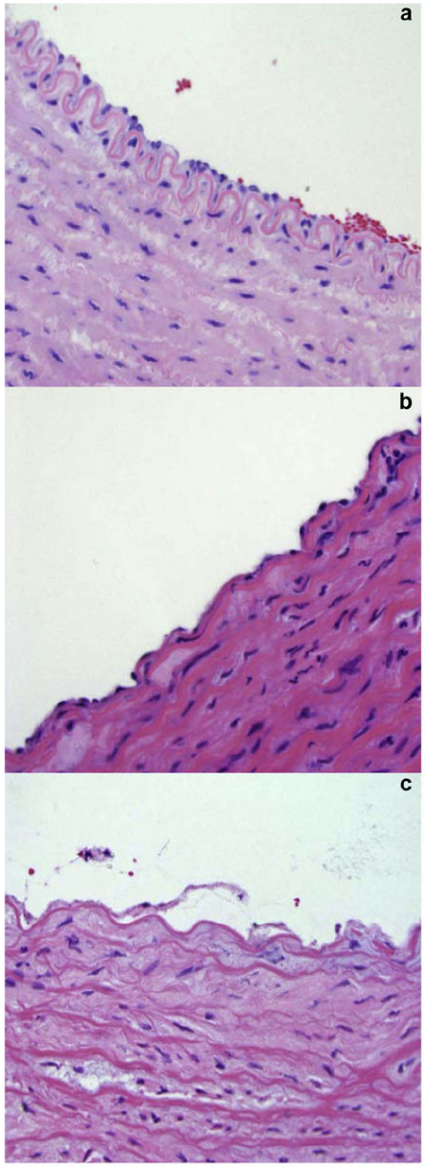

Fig. 7.

Representative microscopic images showing the endothelial and medial layers from carotid arteries of this study. After placement in the *ex vivo* flow system, most arteries showed overall normal aspect (a) with some areas of endothelial cell loss (b). Approximately 10% of the arterial rings showed signs of more severe distress, such as endothelial desquamation and medial edema (c).

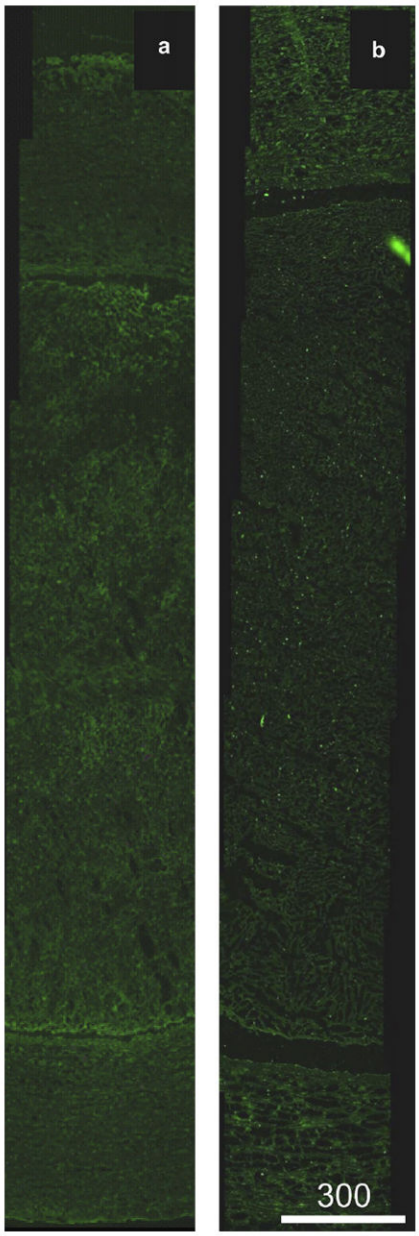

Fig. 8.

Representative fluorescence images of anti–t-PA-labeled arteries with luminal clot. (a) Clot treated with rt-PA (7.1 ± 3.8 μg/mL) and Definity microbubbles (0.79 ± 0.47 μL/mL) in flowing porcine plasma, with ultrasound exposure (120-kHz continuous wave at a 0.44-MPa peak-to-peak pressure amplitude). (b) Clot treated with rt-PA only. Note that although both arteries display abundant autofluorescence, the ultrasound-treated artery does not demonstrate enhanced rt-PA penetration into the arterial tissue.

Table 1

Sample sizes for each treatment combination

	Plasma	Plasma and rt-PA	Plasma and rt-PA with Definity
No ultrasound	7	7	7
With ultrasound	6	5	6

Table 2

Mean total number of particles over 30 min of treatment

Treatments	Size bins		
	2–4 (μm)	4–10 (μm)	10–40 (μm)
	Total particle count ± one standard deviation		
	($\times 10^6$)	($\times 10^6$)	($\times 10^3$)
Naïve porcine plasma	3.4 ± 0.1	0.1 ± 0.1*	2.7 ± 0.6
Control	19.4 ± 17.2	2.0 ± 1.2*,†	8.4 ± 5.3
rt-PA	10.3 ± 5.8	2.3 ± 3.2	2.4 ± 1.7
rt-PA + Definity	6.2 ± 7.8	3.6 ± 3.9	4.6 ± 7.3
US	8.7 ± 1.3	6.5 ± 2.3†	5.6 ± 1.6
rt-PA + US	13.1 ± 11.4	2.9 ± 1.1	4.5 ± 2.6
rt-PA + Definity + US	13.7 ± 5.9	13.1 ± 13.2	6.1 ± 3.7

*,† Pairs of datasets that show statistically significant differences.